

OPEN

Effect of nicotine on *Staphylococcus aureus* biofilm formation and virulence factors

Le Shi^{1,7}, Yang Wu^{2,7}, Chen Yang^{3,7}, Yue Ma¹, Qing-zhao Zhang¹, Wei Huang⁴, Xiao-yi Zhu², Ying-jie Yan², Jia-xue Wang⁵, Tao Zhu⁶, Di Qu^{2*}, Chun-quan Zheng^{1*} & Ke-Qing Zhao^{1*}

Staphylococcus aureus is a common pathogen in chronic rhinosinusitis (CRS) patients, the pathogenesis of which involves the ability to form biofilms and produce various virulence factors. Tobacco smoke, another risk factor of CRS, facilitates *S. aureus* biofilm formation; however, the mechanisms involved are unclear. Here, we studied the effect of nicotine on *S. aureus* biofilm formation and the expression of virulence-related genes. *S. aureus* strains isolated from CRS patients and a USA300 strain were treated with nicotine or were untreated (control). Nicotine-treated *S. aureus* strains showed dose-dependent increases in biofilm formation, lower virulence, enhanced initial attachment, increased extracellular DNA release, and a higher autolysis rate, involving dysregulation of the accessory gene regulator (Agr) quorum-sensing system. Consequently, the expression of autolysis-related genes *lytN* and *atlA*, and the percentage of dead cells in biofilms was increased. However, the expression of virulence-related genes, including *hla*, *hly*, *pvl*, *nuc*, *ssp*, *spa*, *sigB*, *coa*, and *crtN* was downregulated and there was reduced bacterial invasion of A549 human alveolar epithelial cells. The results of this study indicate that nicotine treatment enhances *S. aureus* biofilm formation by promoting initial attachment and extracellular DNA release but inhibits the virulence of this bacterium.

Chronic rhinosinusitis (CRS) is an inflammatory condition affecting the nose and nasal sinuses with a high worldwide prevalence¹. Although CRS represents a considerable health burden and causes a significant reduction in the quality of life, the treatment strategies for CRS are still limited. This is partly because the mechanisms underlying the disease pathology are not well understood. Recently, the contribution of chronic bacterial infections involving biofilms in CRS pathology has been recognized².

Biofilms are communities of bacteria retained within a microbial-derived matrix, which facilitates their survival. Mature biofilms are composed of bacteria, extracellular polysaccharide, extracellular DNA (eDNA), and proteins³. Given their high degree of resistance to the human immune system and the latest antibiotics, bacterial biofilms play an important role in the pathogenesis of many chronic human infections⁴. In 2004, Palmer *et al.* first reported the existence of biofilms on the sinus mucosa of patients with recalcitrant CRS⁵. Numerous studies have subsequently indicated the possible role of bacterial biofilms in CRS.

Tobacco smoke is an important threat to global health⁶. Despite intensive public health interventions, smoking rates are still very high worldwide⁷. Tobacco smoke has been reported to be correlated with CRS and poor sinus surgery outcomes^{8,9}. However, whereas the impact of tobacco smoke on the human body has been studied extensively, the impact of smoke on the microbiome has been relatively less well studied. Increasing evidence indicates that tobacco smoke augments biofilm formation in multiple pathogenic bacteria^{10–13}. In our previous study, we also demonstrated that cigarette smoke can enhance bacterial biofilm formation in multiple bacterial strains isolated from CRS patients¹⁴. However, our understanding of tobacco-induced bacterial biofilms is currently inadequate¹⁵.

¹Department of Otorhinolaryngology and Head and Neck Surgery, Eye & ENT Hospital, Shanghai Key Clinical Disciplines of Otorhinolaryngology, Shanghai Medical College, Fudan University, Shanghai, P.R. China. ²Key Laboratory of Medical Molecular Virology (MOE/NHC/CAMS), Department of Medical Microbiology and Parasitology, School of Basic Medical Sciences, Shanghai Medical College, Fudan University, Shanghai, P.R. China.

³Department of Otolaryngology & Head and Neck Surgery, Ruijin Hospital, Shanghai Jiao Tong University School of Medicine, Shanghai, P.R. China. ⁴Medical Clinic, Hangzhou Haiqin Sanatorium, Hangzhou, Zhejiang, P.R. China.

⁵Department of Laboratory Medicine, Hangzhou Medical College, Hangzhou, Zhejiang, P.R. China. ⁶Department of Preclinical Medicine, Wannan Medical College, Wuhu, P.R. China. ⁷These authors contributed equally: Le Shi, Yang Wu and Chen Yang. *email: dqu@shmu.edu.cn; zhengcq96@163.com; rhinoresearch@163.com

Staphylococcus aureus is a common pathogen that plays a vital role in the condition of CRS patients due to its virulence and its ability to form biofilms¹⁶. Here, we examined the effect of nicotine—one of the most important components of tobacco—on *S. aureus* biofilm formation and virulence-related gene expression. Furthermore, we studied the mechanisms underlying this effect. The findings of this research will potentially contribute to enhancing our knowledge of tobacco smoke-induced bacterial biofilm formation and provide important information for developing novel therapeutic approaches for CRS.

Results

Nicotine enhances *S. aureus* biofilm formation. In order to determine the influence of nicotine on *S. aureus* biofilm formation, we examined the effects of nicotine on seven biofilm-positive clinical *S. aureus* strains collected from the middle meatus of CRS patients as well as that of USA300 strain FPR3757. After incubating bacteria with nicotine for 24 h, there was a significant increase in the amount of biofilm produced by all strains, as determined using a microtiter plate assay (OD₅₇₀). A dose-dependent effect of nicotine on *S. aureus* biofilm formation was observed, and different clinical strains exhibited maximal increases in biofilm formation at different concentrations of nicotine (Fig. 1A). In the case of the USA300 strain, a dose-dependent increase in biofilm formation was observed between 100 µg/mL and 2 mg/mL nicotine, with a maximal increase at 2 mg/mL (Fig. 1B) and a subsequent decrease at higher concentrations (data not shown). Thus, based on these observations and the findings of previous studies^{17,18}, a nicotine concentration of 2 mg/mL was used in all the subsequent experiments to examine the mechanisms underlying nicotine-induced biofilm formation and virulence expression. Confocal laser-scanning microscopy (CLSM) was used to investigate the effect of nicotine on USA300 biofilm formation by measuring the thickness of 24 h mature biofilms, representative images of which are shown in Fig. 1C. The confocal microscopy measurements of biofilm thickness revealed that a dense biofilm had formed in the nicotine-treated group (16.90 ± 0.66 µm, n = 3), compared with the control group (12.67 ± 0.91 µm, n = 3) (*p* < 0.05) (Fig. 1D). Furthermore, we analyzed the effects of nicotine on *S. aureus* growth in response to different concentrations, and accordingly found that higher concentrations promoted a slower growth rate in the exponential phase (Fig. 1E).

Nicotine treatment strengthens *S. aureus* initial attachment but has no effect on poly-*N*-acetylglucosamine polysaccharide synthesis. Bacterial attachment is the initial step of biofilm formation, and in this regard, our results indicated that after treatment with 2 mg/mL nicotine, a larger number of cells of USA300 strain FPR3757 had adhered to the bottom of polyethylene wells (3.44 ± 0.36 × 10⁵, n = 3), compared with the untreated control cells (2.25 ± 0.57 × 10⁵, n = 3) (*p* < 0.05) (Fig. 2A). Fibronectin-binding protein A (FnbA), which is a key surface-attached proteins and ECM-binding protein homologue (Ebh), a giant cell wall-related protein associated with virulence, are both key surface proteins, and therefore we examined the transcription level of these genes during the initial period of biofilm formation (2 h) in response to nicotine treatment. The results indicated that expression of the *fnbA* gene was increased whereas that of *ebh* was decreased after 2 h compared with the control group. (Fig. 2B) Furthermore, to examine the effects of nicotine on bacterial intercellular adhesion, we determined the synthesis of poly-*N*-acetylglucosamine polysaccharide (PIA) by CLSM. Observations indicated that the levels of PIA did not differ significantly between the nicotine-treated and non-nicotine-treated groups (Fig. 2C).

Nicotine promotes the autolysis of *S. aureus*. A Triton X-100-induced autolysis assay was performed to determine the effect of nicotine on autolysis of the *S. aureus* USA300 strain. As shown in Fig. 3A, the bacterial cultures treated with 2 mg/mL nicotine exhibited a significantly higher rate of autolysis than the control group culture. Consistently, the expression of autolysis-related genes, including *lytN* and *atlA*, were found to be upregulated in the nicotine-treatment group (Fig. 3B).

Next, we performed CLSM to examine the 24 h biofilms of nicotine-treated USA300 cells, using LIVE/DEAD staining, the viable cells of which were stained by green fluorescence (SYTO9) and dead cells by red fluorescence (PI). A merged image of the two staining patterns is shown in Fig. 4A. The ratio of red fluorescence intensity to total fluorescence intensity was 41.94% ± 2.00% and 26.39% ± 4.09% (n = 3, *p* < 0.05) in the nicotine-treatment group and the control group, respectively; while the overall green fluorescence intensity in the two groups was 980.3 ± 12.34 and 819.3 ± 33.35 (*p* < 0.05), respectively (Fig. 4B).

Nicotine facilitates eDNA release by *S. aureus*. The upregulation of autolysis is invariably associated with a higher release of eDNA. Thus, we evaluated the eDNA in 24 h *S. aureus* biofilms in the presence and absence of nicotine by staining with PI. The results accordingly revealed that the amount of eDNA (indicated by fluorescence intensities at a wavelength of 610 nm per OD₆₀₀) was higher in the nicotine treatment group (15.95 ± 1.64, n = 3) compared with the control group (10.59 ± 0.51, n = 3) (*p* < 0.05) (Fig. 5).

DNase I and Proteinase K inhibit nicotine-induced biofilm formation. To evaluate whether enhanced biofilm formation is associated with an increase in eDNA release, we observed the effect of DNase I on biofilm formation in the USA300 strain with or without 2 mg/mL nicotine treatment. The results showing that OD₅₇₀ was reduced from 1.506 ± 0.04 to 0.450 ± 0.07 in the nicotine-treated group and from 0.720 ± 0.14 to 0.328 ± 0.05 in untreated group, indicating that nicotine-induced biofilm formation is sensitive to DNase I (25 U/well) (Fig. 6A).

Furthermore, we also investigated whether the enhanced biofilm formation induced by nicotine can be inhibited by Proteinase K (2 µg/mL), and accordingly found that Proteinase K has a suppressive effect on biofilm formation, with OD₅₇₀ values in the nicotine treated group decreasing from 1.300 ± 0.06 to 0.393 ± 0.02 (n = 3, *p* < 0.05), and those in the control group decreasing from 0.721 ± 0.14 to 0.316 ± 0.08 (n = 3, *p* < 0.05) (Fig. 6B).

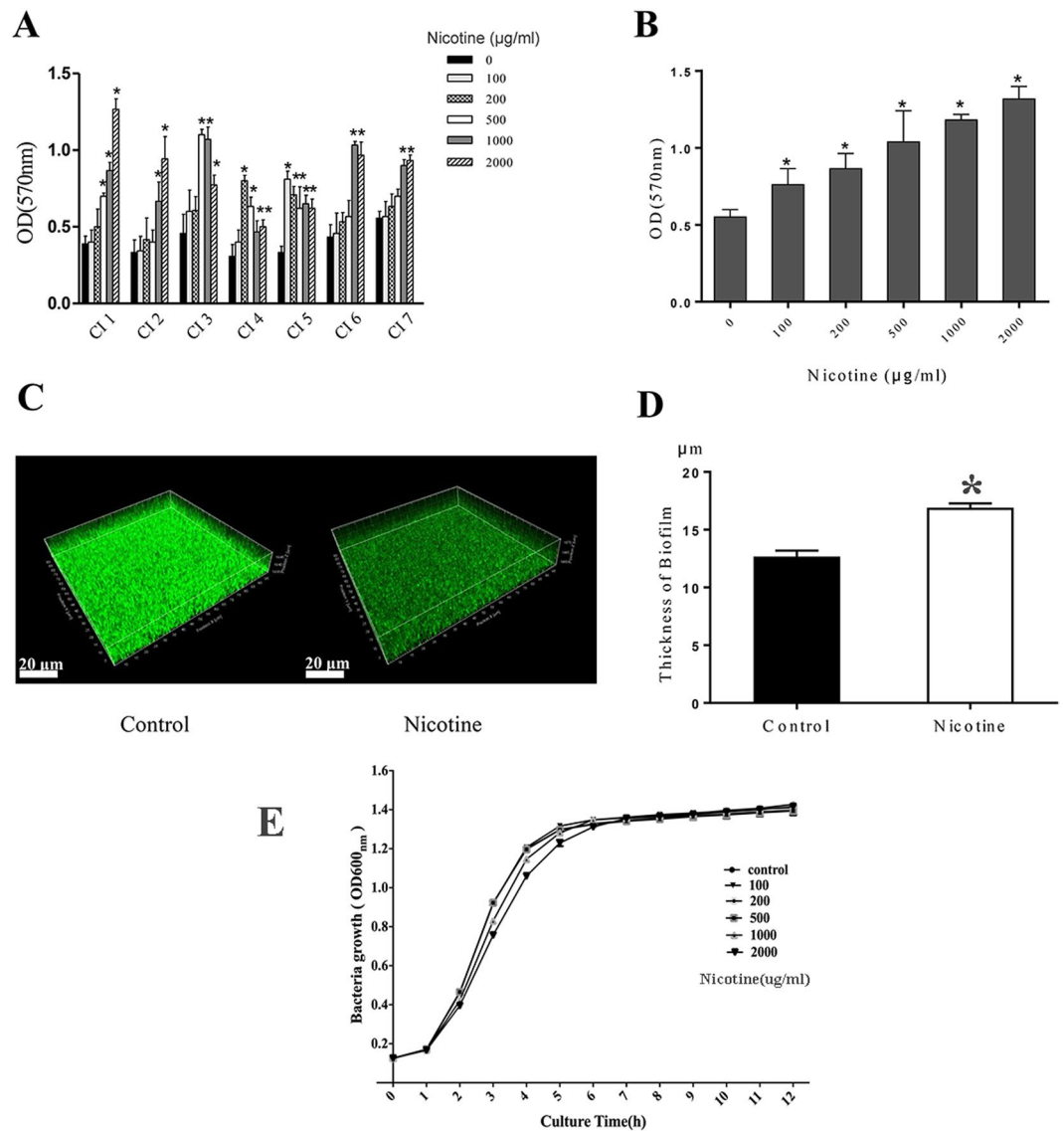


Figure 1. Nicotine induced biofilm formation in *Staphylococcus aureus*. **(A)** Clinical *S. aureus* strains were exposed to various concentrations of nicotine (0, 0.1, 0.2, 0.5, 1, 2 mg/mL). Crystal violet staining of biofilm-associated biomass revealed that the biofilm formation was increased in all strains in response to nicotine treatment. **(B)** A dose-dependent increase in biofilm formation was observed in USA300. Maximal biofilm formation was observed at 2 mg/mL. **(C)** Representatives of confocal images showed that denser biofilms were formed in the nicotine-treated group than in the control group. **(D)** The average thickness of biofilms in nicotine treatment group was $16.90 \pm 0.66 \mu\text{m}$ ($n = 3$), while the thickness in the untreated group was $12.67 \pm 0.91 \mu\text{m}$ ($n = 3$) ($p < 0.05$). **(E)** *S. aureus* USA300 strain FPR3757 growth curves under different concentrations of nicotine (0, 0.1, 0.2, 0.5, 1, 2 mg/mL) were determined by measuring the OD at a wavelength of 600 nm at 1-h intervals for 12 h. $*P < 0.05$ compared with untreated group. CI, clinical isolates.

Nicotine treatment suppresses *S. aureus* virulence. As one of the major human pathogens, *S. aureus* can produce numerous virulence factors, including alpha hemolysin (*hla*) and beta hemolysin (*hlyB*), responsible for hemolysis; nuclease (*nuc*), serine protease (*ssp*), and surface proteins A (*spa*), and genes responsible for pigmentation, including *sigB*, *rsbU* (global regulators), *citZ*, and *crtN*¹⁹. We examined the effects of nicotine on the expression levels of these virulence genes in the *S. aureus* USA300 strain using qRT-PCR. The results showed that in the nicotine treatment group, expression of the virulence-related genes *hla*, *hlyB*, *pvl*, *nuc*, *ssp*, *spa*, and *sigB* was downregulated at both 12 h and 24 h, the expression of *rsbU* decreased at 12 h, whereas only the coagulase gene *coa* and the pigmentation-related gene *crtN* was downregulated at 24 h (Fig. 7A).

To investigate whether the altered gene expression patterns affected the virulence-related phenotypes, the hemolysis (24 h) and carotenoid pigmentation formation (24 h) of USA300 cells were investigated in the presence and absence of nicotine (2 mg/mL). As expected, the hemolysis and pigmentation phenotypes were altered upon treating with nicotine. A clear/complete hemolytic ring (β -hemolytic phenotype) was observed around USA300

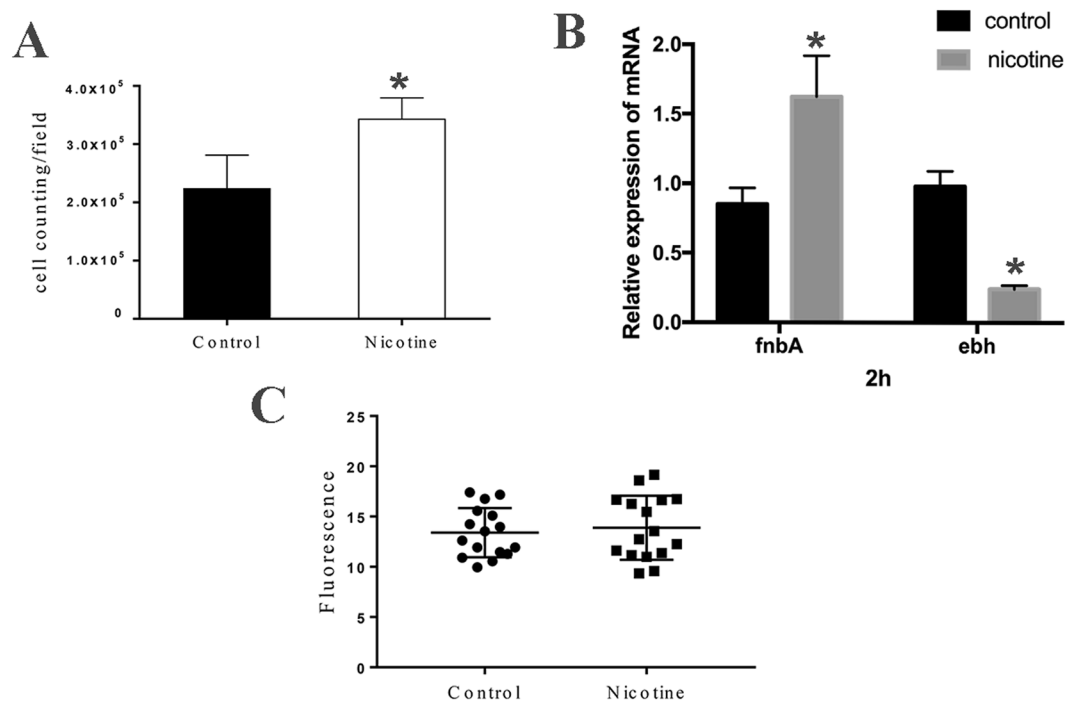


Figure 2. Nicotine increased *S. aureus* attachment and polysaccharide intercellular adhesin (PIA) production. (A) The number of attached bacteria was counted and analyzed. More attached cells were observed in the nicotine-treated group ($3.44 \pm 0.36 \times 10^5$, $n = 3$) than in the control ($2.25 \pm 0.57 \times 10^5$, $n = 3$). (B) Transcriptional levels of the *fnbA* and *ebh* genes in *S. aureus* USA300 strain cultured in TSB and TSB supplemented with 2 mg/mL nicotine for 2 h were detected by qRT-PCR ($n = 3$). (C) The levels of PIA were detected by CLSM. No significant difference between the nicotine treatment and control groups. * $P < 0.05$ compared with untreated group.

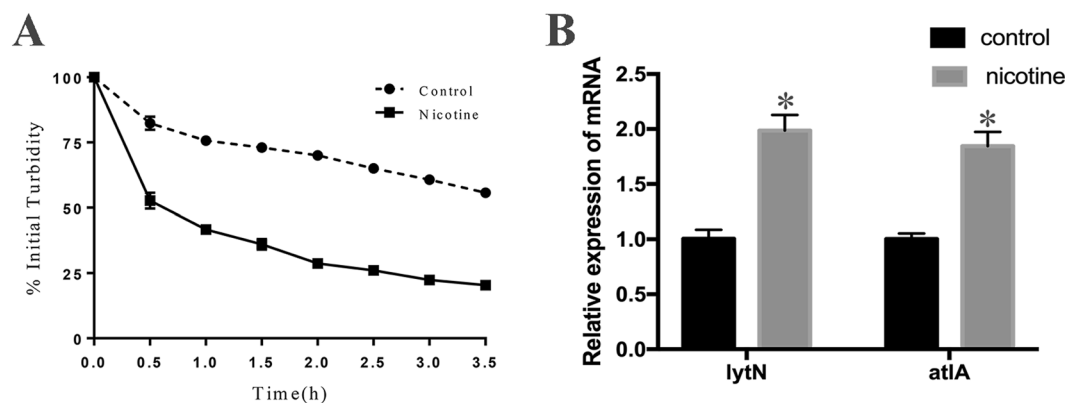


Figure 3. Nicotine increased *S. aureus* autolysis rate. (A) The mid-log phase culture ($OD_{600} = 0.6$) was collected and then resuspended in the same volume of 0.05 M Tris-HCl (pH 7.2) containing 0.05% Triton X-100, the solution was incubated at 30 °C and OD_{600} was measured every 30 min. The rate of autolysis was measured as the decline in optical density. (B) Transcriptional levels of the autolysis-related genes *lytN* and *atlA* in *S. aureus* USA300 strain cultured in TSB and TSB supplemented with 2 mg/mL nicotine detected by qRT-PCR ($n = 3$). Data were represented as mean \pm SD of three independent experiments. * $P < 0.05$ compared with untreated group.

colonies on blood agar plates, whereas a smaller β -hemolytic ring was formed on the blood agar plate containing nicotine (Fig. 7B). Compared with the control cells, USA300 cells cultured in TSB medium supplemented with 2 mg/mL nicotine for 24 h showed visually reduced pigment production, whose absorbance at OD_{462} decreased from 0.263 ± 0.01 in the non-nicotine treated group to 0.119 ± 0.01 in the nicotine-treated group ($n = 3$, $p < 0.05$), thereby indicating that nicotine suppresses bacterial virulence (Fig. 7C).

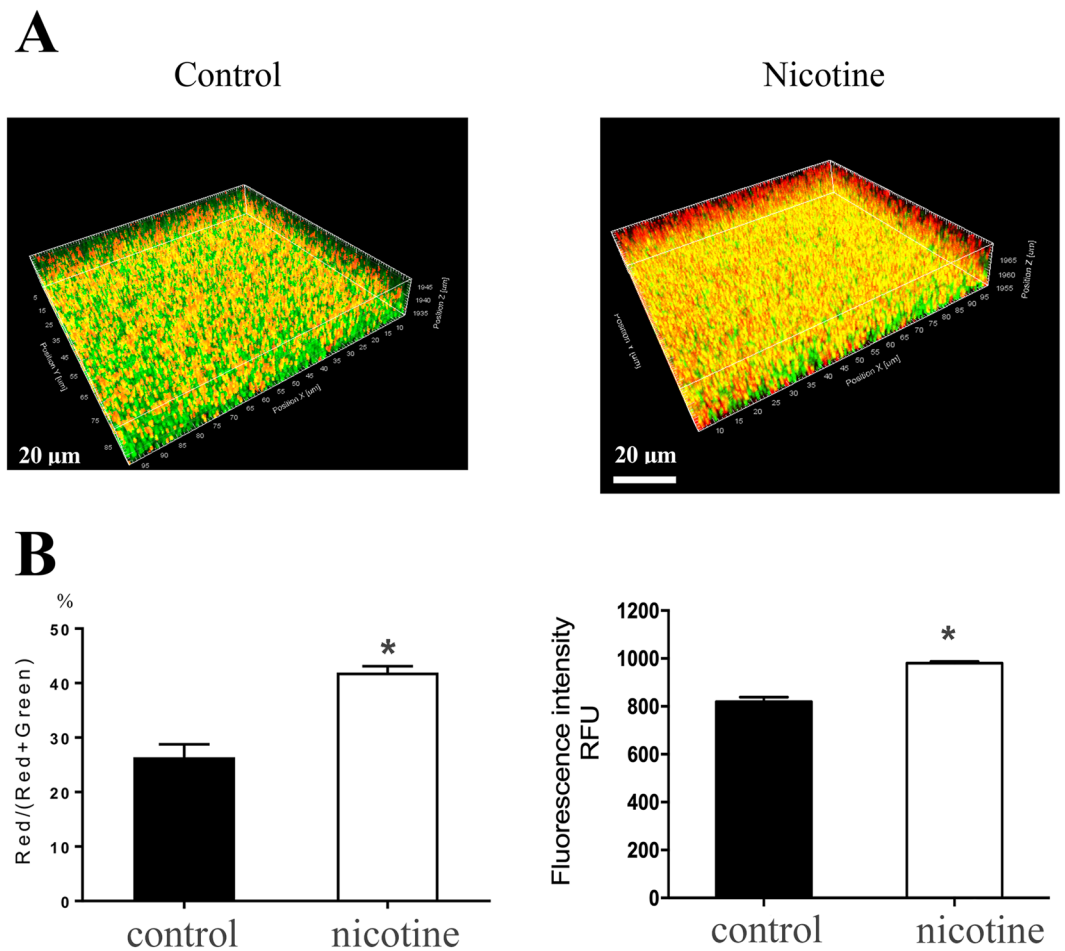


Figure 4. More dead cells were observed after nicotine treatment. Biofilms were grown for 24 h with or without 2 mg/mL nicotine ($n=3$), then stained with SYTO9 (green fluorescence) and PI (red fluorescence) to represent the live and dead bacteria independently. (A) Biofilms were observed using CLSM with a 63×1.4 -NA oil immersion objective. (B) Fluorescence was quantified using Leica Application Suite 1.0 software. A higher overall green fluorescence intensity was observed in the nicotine treated group. $*P < 0.05$. RFU, Relative fluorescence units.

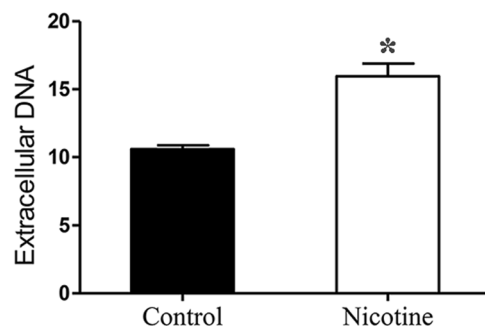


Figure 5. Nicotine enhanced the release of extracellular DNA (eDNA). The amount of eDNA in the matrix of *S. aureus* biofilm (24 h) were determined by measuring the fluorescence of PI-bound eDNA with the excitation/emission wavelength at 535/610 nm. Relative amount of eDNA was expressed as the fluorescence intensity per OD_{600} unit. The amount of eDNA was higher in the nicotine treatment group (15.95 ± 1.64 , $n=3$) as compared to the control group (10.59 ± 0.51 , $n=3$) $*P < 0.05$.

Nicotine attenuates the capacity of *S. aureus* to invade epithelial cells. Epithelial cells are the first-line defense against disease-causing organisms, and ability of bacteria to invading these cells is a facet reflecting the virulence of these organisms. To further elucidate the effect of nicotine on the virulence of *S. aureus*, we

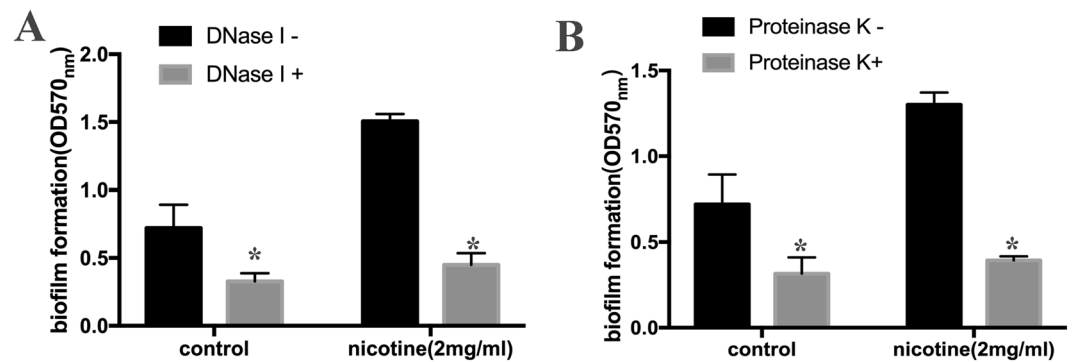


Figure 6. DNase I and Proteinase K inhibit nicotine-induced biofilm formation. The biofilm formation of *S. aureus* USA300 strain was detected using a microtiter plate assay by measuring crystal violet stained biofilm at OD570. DNase I (25 U/well) and Proteinase K (2 ug/ml) was added to the well in both 2 mg/ml nicotine treatment group and control group. (A) Treated by DNase I, the average thickness of biofilms varied from 1.506 ± 0.04 to 0.450 ± 0.07 in the nicotine-treated group ($n = 3$) and from 0.720 ± 0.14 to 0.328 ± 0.05 in untreated group. ($n = 3$) (B) Proteinase K (2 ug/ml) disrupted biofilm formation, in the nicotine treated group decreasing from 1.300 ± 0.06 to 0.393 ± 0.02 ($n = 3$), and in the control group decreasing from 0.721 ± 0.14 to 0.316 ± 0.08 ($n = 3$). * $P < 0.05$.

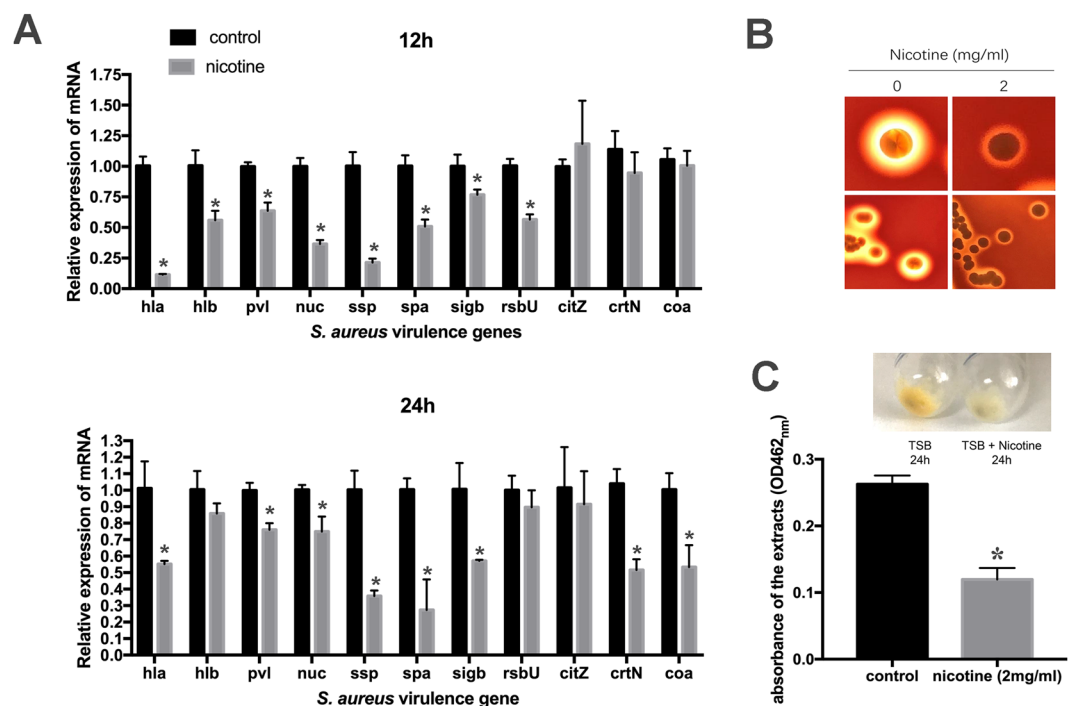


Figure 7. Nicotine treatment suppresses *S. aureus* virulence. (A) Transcriptional levels of the virulence genes in *S. aureus* USA300 strain cultured in TSB and TSB supplemented with 2 mg/mL nicotine for 12 h/24 h were detected by qRT-PCR ($n = 3$). In the nicotine-treatment group, the expression of the virulence genes, *hla*, *hlb*, *pvl*, *nuc*, *ssp*, *spa*, *sigB* was downregulated at both 12 h and 24 h, while expression of the coagulase gene *coa* and the pigmentation-related gene *crtN* was downregulated at 24 h. (B) The *S. aureus* USA300 strain was inoculated on normal blood agar plates (left) and blood agar plates containing 2 mg/mL nicotine (right), respectively. After incubation at 37 °C for 24 h, a smaller β -hemolytic ring (β -hemolytic phenotype) was formed on the blood agar plate containing nicotine than the control. (C) Nicotine treatment suppressed carotenoid pigment formation. The *S. aureus* USA300 strain was cultured for 24 h in TSB (left) and TSB supplemented 2 mg/mL with nicotine (right) respectively. The pigment formed by bacterial cell pellets in nicotine group was reduced as compared to the control. Pigment production was quantified at OD₄₆₂, decreasing from 0.263 ± 0.01 in the control group ($n = 3$) to 0.119 ± 0.01 in the nicotine-treated group ($n = 3$). These photos are representative of three independent experiment.

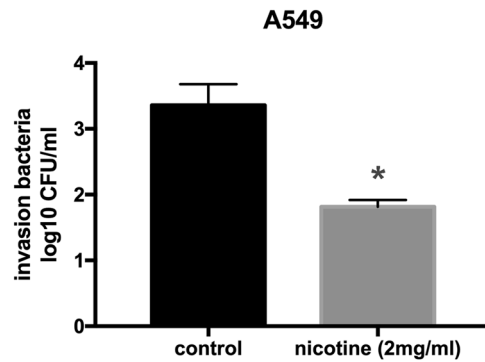


Figure 8. Nicotine treatment inhibits *S. aureus* invasion in A549 epithelial cells. Cell monolayers were infected with a bacterial multiplicity of infection (MOI) of 10:1. After 2 h of incubation, 200 µg/mL Gentamicin and 40 µg/mL Lysostaphin was added to kill the bacteria external to the monolayer cells at 37 °C in 5% CO₂ for 30 min. Then the monolayer cells were subsequently lysed with 200 µL 0.1% Triton X-100 for 20 min at room temperature, and were then diluted with PBS and plated on TSB-agar plates to determine the number of intracellular bacteria. Intracellular CFUs in nicotine treated group and control group were $3.360 \pm 0.25 \log^{10}$ and $1.816 \pm 0.08 \log^{10}$ respectively. ($n = 3, p < 0.05$) Data were represented as mean \pm SD of three independent experiments. * $P < 0.05$.

investigated the capacity of *S. aureus* to invade A549 human alveolar epithelial cells. Our results showing CFUs of $3.360 \pm 0.25 \log^{10}$ and $1.816 \pm 0.08 \log^{10}$ ($n = 3, p < 0.05$) for the control and nicotine-treated groups intracellularly respectively, indicated that nicotine inhibited the ability of these bacteria to invading A549 cells (Fig. 8).

Nicotine affects biofilm formation in *S. aureus* in an accessory gene regulator-dependent manner.

Previous studies have indicated that the activity of the accessory gene regulator (Agr) system appears to have an influence on *S. aureus* virulence and enhance biofilm formation by this bacterium^{20–22}. In this study, we explored the expression of Agr system genes (*agrA*, *agrB*, *agrC*, and *agrD*) at 2 h and 24 h during the biofilm formation process in the presence or absence of nicotine. The results showed that expression of *agrA*, *agrB*, *agrC*, and *agrD* in the nicotine-treated group were lower than those in the control group, ($n = 3, p < 0.05$), and that the expression appeared to be both time- and dose-dependent. Figure 9A shows that gene expression gradually decreased from 0 h to 2 h and 2 h to 24 h. Furthermore, at 24 h, we found that the degree of reduction in the 2 mg/mL group was more pronounced than that in the 1 mg/mL group (Fig. 9B).

In addition, we investigated whether the strengthened initial attachment due to nicotine exposure was a result of Agr dysfunction. By observing the effect of nicotine on USA300 FPR3757 mutants harboring transposon insertions in the *agrA* and *agrC* genes, we found that nicotine-induced enhancement of the initial attachment stage was abrogated in these two mutant strains, indicating that the Agr system is involved in the nicotine-potentiated initial attachment process (Fig. 9C).

Discussion

Given that *S. aureus* is a frequent colonizer of the nasal mucosa and lower respiratory tract passages, it will be exposed to cigarette smoke during smoking. Previous studies have indicated that an extract of cigarette smoke induces biofilm formation in various bacterial species and that nicotine enhances biofilm formation by *Streptococcus mutans*, *Streptococcus gordonii* and *Staphylococcus epidermidis*^{17,23–25}. In the present study, we found that nicotine can enhance *S. aureus* biofilm formation capability in both clinical *S. aureus* strains and USA300 strain FPR3757. We hypothesize that the nicotine-induced enhancement of *S. aureus* biofilm formation may be a general phenomenon and that it might represent a protective reaction on the part of *S. aureus* to adverse environments, such as exposure to nicotine. Under adverse conditions, *S. aureus* develops a defense phenotype biofilm by altering gene expression, which results in the bacteria becoming embedded in a protective biofilm that renders them less susceptible to eradication.

In the current study, we found that nicotine treatment enhances *S. aureus* biofilm formation by increasing initial attachment and the release of extracellular DNA, although it also attenuates bacterial virulence, including inhibition of the expression of major virulence-related genes, reducing pigment production, and reducing bacterial invasion of epithelial cells, the latter of which is a pathological process related to activity of the Agr system.

Nicotine is one of the most toxic chemicals in tobacco. Huang *et al.*¹⁷ mentioned that high levels of nicotine of up to 2.3 mg/mL are detected in the saliva of smokers. Although to date there have been no data published regarding nicotine concentrations in nasal mucus, several facts indicate that these concentrations could be similar to the levels of nicotine in saliva. Firstly, the nose is one of the most exposed organs to smoke and the nasal mucosa is one of the major routes via which nicotine is absorbed from tobacco²⁶. Secondly, the nasal and oral cavities are interconnected, and are hence simultaneously exposed to nicotine during smoking. Thus, levels of nicotine in nasal mucus may reach concentrations in the range of that which we used in the present study (2 mg/mL) to investigate the underlying mechanism of nicotine-induced biofilm formation and virulence expression *in vitro*.

Biofilm formation proceeds in two steps, namely, an initial bacterial adhesion followed by cell proliferation and aggregation²⁷. The essential step in the establishment of any *Staphylococcus* infection is the attachment to host

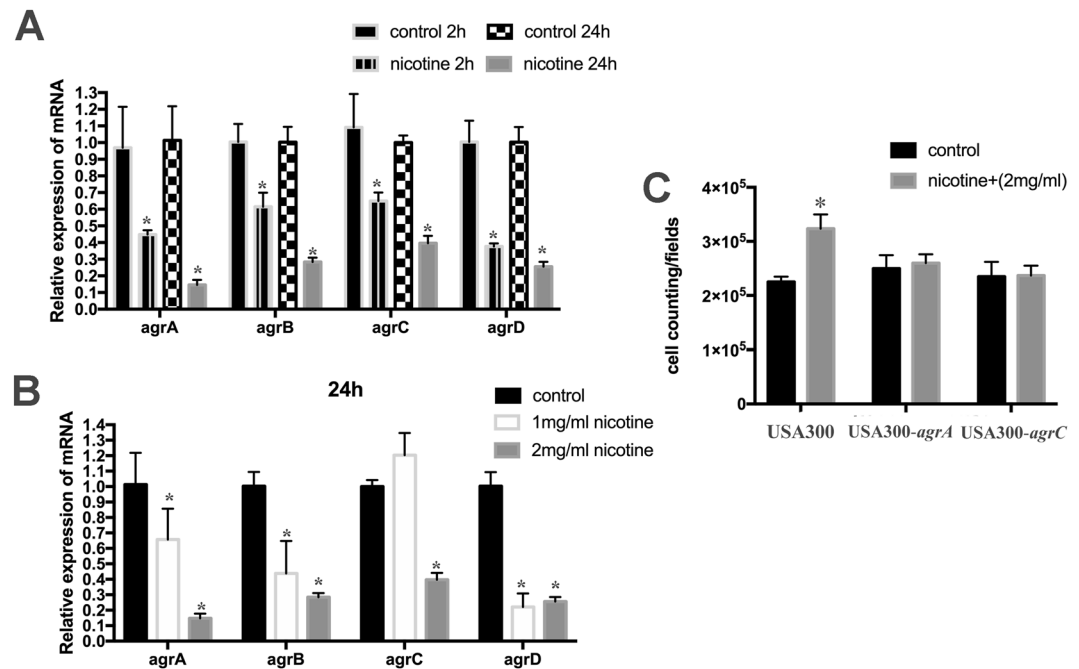


Figure 9. Agr system plays a role in biofilm development induced by nicotine. (A) The relative mRNA expression of Agr system genes (*agrA*, *agrB*, *agrC*, and *agrD*) was evaluated at 2 h and 24 h during the biofilm formation process in the presence or absence of nicotine. (B) The relative mRNA expression of *agrA*, *agrB*, *agrC*, and *agrD* genes were detected when treated with 0, 1 mg/ml, 2 mg/ml nicotine at 24 h. (C) The number of attached bacteria was counted and analyzed in USA300, USA300-*agrA*, USA300-*agrC*. The nicotine-induced enhancement of the initial attachment stage was abolished in these two mutant strains. Data were represented as mean \pm SD of three independent experiments. * $P < 0.05$.

tissues. We observed that a larger number of bacteria were attached to the polyethylene surface of culture plate wells in a nicotine-treated group than in a control group, thereby indicating that nicotine may enhance the initial step in *S. aureus* biofilm formation. These results are consistent with the findings of Cogo *et al.*, who demonstrated that cotinine, the predominant nicotine metabolite, enhances the adhesion of *Porphyromonas gingivalis* to epithelial cell monolayers²⁸. Surface proteins are the main components involved in biofilm formation, particularly during initial attachment^{29,30}. *FnbA* is a well-known surface protein associated with the attachment stage of biofilm formation and *Ebh* is a giant protein found on the surface of *S. aureus*. In infected mice, *ebh* variants have been shown to be associated with the diminished virulence of *S. aureus*³¹. In response to nicotine treatment (2 h), we found that transcription levels of *fnbA* were increased, whereas the expression of *ebh* decreased. Furthermore, expression of the autolysis-related gene *atlA*, which is also associated with initial attachment, was also found to be increased.

The staphylococcal biofilm matrix has been reported to contain eDNA proteins, and polysaccharides, and we found that compared with the control group, larger amounts of eDNA were present in the matrix of *S. aureus* biofilms in the nicotine-treated group. Consistent with the findings of Kulkarni *et al.*¹⁰, we observed that the enhanced biofilm formation promoted by nicotine was suppressed by DNase I and proteinase K, thereby providing evidence that eDNA and proteins may play key roles in the nicotine-induced enhancement of initial attachment. Cell autolysis is a major source of eDNA in biofilms and a previous study has demonstrated that such autolysis could have a significant impact on biofilm formation^{32,33}. Thus, we speculated that nicotine might increase *S. aureus* autolysis. However, results from previous studies to determine the effect of CS on bacterial autolysis are not always consistent: MacEachern³⁴ observed that exposure of *S. aureus* USA300 to CS resulted in an increased resistance to Triton-induced lysis, as a consequence of cell wall alteration, including changes in surface charge and hydrophobicity, Kulkarni *et al.* found DNase I inhibited CS-induced biofilm formation and observed 6-fold increase of autolysis associated gene, *cidA*, in USA300. We found that nicotine significantly increased *S. aureus* autolysis compared with the control group.

It has previously been shown that *S. aureus* biofilm formation is tightly regulated by a quorum sensing system, accessory gene regulator (Agr) system²⁰, encoded by *agrBDCA* operon. The *agrC/agrA* two-component system negatively regulates *S. aureus* biofilm formation, partially by increasing extracellular protease production and inhibiting cell adhesion to surfaces. Our real-time PCR analysis revealed that transcription of the *agr* operon (*agrA*, *agrB*, *agrC*, and *agrD*) showed a marked decrease in expression in the nicotine treatment group (at 2 h and 24 h) depending on nicotine concentration and time exposure. Furthermore, we found that in USA300 mutants harboring a transposon insertion in either the *agrC* or *agrA* gene, the nicotine-induced increase in initial attachment was abolished. Taken together, our observations indicated that the augmentation of biofilm formation by nicotine may be directly or indirectly related to downregulation of the Agr system.

Stains	Description	Source or Reference
USA300 FPR3757	a MRSA strain (GenBank Accession Number: NC 007793)	³⁹
USA300- <i>icaA</i>	USA300 FPR3757 with a transposon insertion in the <i>icaA</i> gene	This study
USA300- <i>agrA</i>	USA300 FPR3757 with a transposon insertion in the <i>agrA</i> gene	This study
USA300- <i>agrC</i>	USA300 FPR3757 with a transposon insertion in the <i>agrC</i> gene	This study

Table 1. Bacterial strains used in this study.

As one of the major human pathogens, *S. aureus* can produce numerous virulence factors, whose expression is influenced by the microenvironment in the human body and is related with the process of bacterial pathogenesis. For example, it has been reported that α -toxin (α -hemolysin), a major cytolytic toxin expressed by the majority of *S. aureus* clinical isolates, is associated with the persistence of *S. aureus* cells in tissues and can also provoke cellular responses in nasal polyp cells from CRS patients, therefore, may play a role in the pathophysiology of CRS³⁵. Although excess expression of virulence factors including exotoxins may enhance bacterial pathogenicity in the host, it can trigger augmented immune responses, which may lead to acute inflammations, hypersensitivity and then quick clearance of bacteria cells. Thus, the transcriptional regulation of virulence genes is vital for bacterial survival and adaption in the host. In *S. aureus*, the Agr system initiates RNAIII transcription and plays a pivotal role in the regulation of myriad virulence factors, especially exotoxin genes³⁶. A recent extensive study conducted by Lacoma *et al.*²⁹ showed that the Agr system mediates CS-induced biofilm augmentation and CS-reduced toxin production. Based on the data in this study and in the literatures, we hypothesize that the presence of nicotine represses the expression of *agrBDCA* operon and thereby may also have an inhibitory effect to various virulence-related genes. In line with the expectation, the virulence genes including *hla* (alpha hemolysin), *hly* (beta hemolysin), *pvl* (leucocidin), *nuc* (thermostable nuclease), *ssp* (serine protease), *spa* (protein A) and the genes responsible for pigmentation, including *sigB*, *rsbU*, *citZ*, and *crtN*¹⁹, showed decreased transcriptional levels in the nicotine treatment group at 12 h or 24 h. Consequently, nicotine treatment inhibited subsequent β -hemolysis on blood agar plates and carotenoid pigment production. Furthermore, using the A549 cell line to assess the invasion ability of *S. aureus* after nicotine treatment, we showed that nicotine decreased the number of intracellular bacteria. We speculate that on one hand, nicotine induces reduction in multiple bacterial virulence genes expression and may hinder the progress of acute infection. On the other hand, it enhances bacterial biofilm formation, which can protect bacteria from the host immune attack and therefore contribute to the persistence of this pathogen.

In conclusion, the results of this study provide further insights into the mechanisms whereby tobacco smoke induces *S. aureus* biofilm formation. We observed that nicotine can enhance biofilm formation in both clinical *S. aureus* strains obtained from CRS patients and the USA300 FPR 3757 strain. The altered biofilm formation was associated with enhanced initial cell attachment, elevated eDNA release, and enhanced *S. aureus* autolysis. Additionally, we found that nicotine repressed transcription of various virulence-related genes and inhibited β -hemolysis on blood agar plates, carotenoid pigment production and invasion in A549 cells by *S. aureus*. We hypothesize that the nicotine-induced reduction in bacterial virulence and enhancement of biofilm formation increases bacterial fitness and strengthens adaption to the harsh nasal environment, thereby may contribute to chronic infection.

Materials and Methods

Ethics statement. All procedures performed in studies involving human participants were in accordance with the ethical standards of the Institutional Review Board of Eye & ENT Hospital (reference number KJ2011-31) and with the 1964 Helsinki Declaration and its later amendments or comparable ethical standards. In addition, informed consent was obtained from all participants.

Bacteria strains and culture media. This study was previously approved by the Ethics Committee on Research of Eye & ENT Hospital. The clinical strains of *S. aureus* were collected during endoscopic surgery performed at the Shanghai Eye and ENT Hospital of Fudan University, and isolated from the middle meatus of CRS patients. The bacterial strains used in this study are listed in Table 1. *S. aureus* USA300 strain FPR3757 and mutants of this strain harboring transposon insertions in the *icaA*, *ebh*, *agrA*, and *agrC* genes were provided by Professor Ying Zhang at Johns Hopkins University. Tryptone soya broth (TSB; Oxoid, USA) was used for bacterial culture, and TSB supplemented with 1% glucose (TSBG) was used for bacterial biofilm formation experiments.

Detection of bacterial biofilm formation. Bacterial strains were grown in TSB with or without nicotine for 6 h at 37°C to obtain bacteria in a mid-exponential phase. The cultures were then diluted 1:200 with TSBG supplemented with or without nicotine, and 200 μ L of bacterial suspension was added to each well of a 96-well microplate and incubated at 37°C for 24 h. To determine the effect of DNase I and proteinase K on biofilm formation, 5 μ L DNase I (5 U/ μ L, Takara, Shanghai, China) and 2 μ g/mL Proteinase K (Sango, Shanghai, China) were added to the wells. Thereafter, the wells were washed three times with phosphate-buffered saline (PBS) to remove unattached bacteria and then 200 μ L of 100% methanol was added to each well to fix the attached cells at room temperature for 20 min. After removal of the methanol, the biofilms were air-dried and stained with 2% crystal violet at room temperature for 8 min. The wells were then washed with running tap water until the water was clear. Subsequently, 200 μ L of 10% acetic acid was added to each well and incubated for 1 h. Finally, the

stained biofilms were quantified by estimating the optical density (OD) at 570 nm using a microtiter-plate reader (DTX 880 Multimode Detector; Beckman Coulter, USA). The *S. aureus* USA300 strain and its isogenic *icaA* gene transposon insertion mutant were used as a biofilm-forming strain and a non-biofilm-forming control strain, respectively.

Bacterial growth curve determination. *S. aureus* growth curves were determined by measuring the OD at a wavelength of 600 nm using an automated growth curve detector (Biocreen C, Finland). Briefly, overnight cultures were diluted (1:200) and incubated in the presence of different nicotine concentration with shaking at 220 rpm and 37 °C. The OD₆₀₀ values of bacterial cultures were measured at 1 h intervals for 12 h.

Observation of *S. aureus* biofilms by confocal laser-scanning microscopy (CLSM). *S. aureus* biofilms were cultured in TSB with or without 2 mg/mL nicotine in glass-bottomed dishes, washed with three times with PBS, and then stained with LIVE/DEAD staining dye [1 μM of SYTO9 and 1 μM of propidium iodide (PI)] for 20 min. The biofilms were observed using a confocal laser-scanning microscope (Leica TCS SP8; Leica Microsystems, Germany) with a × 63 1.4-NA oil immersion objective. Fluorescence was quantified using Leica Application Suite 1.0 software (Leica Microsystem, Germany), and IMARIS 7.0 software (Bitplane, USA) was used to generate three-dimensional images of biofilms.

Initial bacterial attachment assays. Bacteria strains were cultured in TSB with or without 2 mg/mL nicotine to mid-exponential phase, and the bacterial cells were diluted with TSB to OD₆₀₀ = 0.1. The diluted culture was added to cell culture-treated 6-well polystyrene microtiter plates (Nunc, Denmark; 1 mL per well) and incubated at 37 °C for 2 h. Thereafter, the attached cells were washed gently with PBS (three times) and imaged. For each sample, six representative optical fields were randomly selected, and cells were counted using ImageJ software.

Detection of polysaccharide intercellular adhesin (PIA) by spectrofluorometric assay. *S. aureus* biofilms were formed with or without 2 mg/mL nicotine in 96-well polystyrene microplates, washed gently with PBS, and then stained with 200 μL of 5 μg/mL wheat germ agglutinin (WGA)-Alexa Fluor 350 fluorescent conjugate (ThermoFisher, USA). After incubation at 4 °C for 2 h in the dark, the conjugate was removed, and the wells were gently washed three times with PBS. The plate was then air-dried at room temperature for 15 min, following which, 200 μL of 33% acetic acid was added to each well. The biofilms in the wells were incubated at 37 °C for 1 h, scraped thoroughly, and then 150 μL solution from each well was transferred to a solid black microplate (PerkinElmer, USA) for top reading using a Varioskan™ LUX microplate reader (ThermoFisher, USA; fluorescence at λ_{excitation} = 346 nm and λ_{emission} = 442 nm).

Triton X-100-induced bacterial autolysis assay. To determine the effect of nicotine on *S. aureus* autolysis, a Triton X-100-induced autolysis assay was performed. An overnight culture of the *S. aureus* USA300 strain FPR3757 was diluted 1:200 with TSB containing 1 M NaCl, and was then grown with or without 2 mg/mL nicotine to mid-log phase (OD₆₀₀ ~ 0.6). The cells were collected by centrifugation and washed twice in cold sterile PBS. After resuspension in the same volume of 0.05 M Tris-HCl (pH 7.2) containing 0.05% Triton X-100, the solution was incubated at 30 °C and OD₆₀₀ values were measured at 30-min intervals. The autolysis rate was determined by calculating the decline in OD₆₀₀ values. Data are represented as the mean ± SD of three independent experiments.

Detection of extracellular DNA (eDNA). The quantity of eDNA in *S. aureus* cultures was determined using modifications of the methods described by Allesen-Holm *et al.* and Qin *et al.*^{37,38}. Briefly, *S. aureus* strains were cultured overnight in TSB supplemented with or without 2 mg/mL nicotine, following which, the cultures were diluted with minimal growth medium (AB medium) supplemented with 0.5% glucose, 10% TSB, and 0.05 mM PI, to an OD₆₀₀ of 0.001. The diluted cultures were transferred to a 96-well microplate (200 μL per well) and incubated with or without 2 mg/mL nicotine at 37 °C for 24 h. The OD₆₀₀ values were measured using a microplate reader (BioRAD, USA). The fluorescence of PI-bound eDNA was measured at excitation/emission wavelengths of 535/610 nm using a Varioskan™ LUX microplate reader. The relative amount of eDNA was expressed as the fluorescence intensity per OD₆₀₀ units.

RNA extraction. Overnight cultures of USA300 were diluted 1:200 with TSB and incubated with or without 2 mg/mL nicotine at 37 °C to an OD₆₀₀ of 0.6 (mid-log phase). Bacterial cells were collected by centrifugation (4000 × g), washed three times with ice-cold saline, and homogenized using a Beadbeater-16 homogenizer (Biospec, USA). The bacterial RNA was purified using an RNeasy kit (Qiagen, Germany).

Quantitative real-time PCR analysis. The primers used in this study are listed in Table 2. DNase-treated RNA was reverse transcribed (Takara) to cDNA. All samples were prepared in triplicate and then quantified by qPCR using an ABI 7500 real-time PCR system (Applied Biosystems, USA) and SYBR Green I mixture (Takara). The data were normalized using *gyrB* as an internal control.

Analysis of hemolytic phenotype. The *S. aureus* USA300 strain was inoculated on blood agar plates (BioMérieux, China) and blood agar plates containing 2 mg/mL nicotine. The plates were cultured at 37 °C for 24 h, after which the hemolytic phenotype was observed and photographed.

Primers	Sequence (5' → 3')
gyrB-F	ACATTACAGCAGCGTATTAG
gyrB-R	CTCATAGTGATAGGAGTCTTCT
lytN-F	GACACCATTAGTAGAACCAA
lytN-R	AACATTGCCATCCATAAC
atlA-F	AAGTTGTTGTAGTTGATGATGA
atlA-R	TAGTAATACGATGTCTGGTTCT
hla-F	GGTATATGGCAATCAACTT
hla-R	CTCGTTCGTATATTACATCTAT
hly-F	GCACTTACTGACAATAGT
hly-R	GACTAACTAACTTCAAATCAG
pvl-F	TGCCAGTGTATCCAGAG
pvl-R	ATTATTACCTATCCAGTGAAGTTG
nuc-F	GCGATTGATGGTGATACGGTTA
nuc-R	TTAGGATGCTTTGTTTCAGGTGTA
ssp-F	CGGTGTAGTTGTAGGTAA
ssp-R	TTGGATAATTGTCTTGGTTAA
spa-F	AGTGCTAACCTATTGTCAGA
spa-R	ACCATTGCGTTGTTCTTC
sigB-F	GATGAACCTAACCGCTGAAT
sigB-R	TTCCATTGCTTCTAACACTT
rsbU-F	ATAACGATGGCACAATGA
rsbU-R	TGAGTGCCATAAGAATCC
citZ -F	ACCAACAGATATAGAAGTAGAAG
citZ -R	ATGATGATACCGCACAAAC
crtN -F	AATGCTGAACAAGAGTAATC
crtN -R	AGTGAATGGTGACATAAGA
coa -F	CTCAAGGAGAATCAAGTG
coa -R	AATGTTCCATCGTTGTATT
fnbA-F	TTCCTTAACTACCTCTTCT
fnbA -R	CAATCATATAACGCAACAG
ebh-F	GTCAGTCGCATCACCATT
ebh-R	CACAATCATCAATCCAAGCATAT
agrA-F	GCAGTAATTCAGTGATGTTCA
agrA -R	TATGGCGATTGACGACAA
agrB-F	GGTGAATCTCAGTATATGC
agrB-R	GCTTCTATTATGATGCCTAA
agrC-F	GCAGTATTGGTATTATTCTTGA
agrC -R	TGCGTGGTATATCATCAG
agrD-F	ACATCGCAGCTTATAGTA
agrD-R	CGTGTAATTGTGTTAATTCT

Table 2. Primers used in this study.

Cell culture and epithelial cell invasion assay. A549 human alveolar epithelial cells (ATCC CCL185) were cultured in high-glucose Dulbecco's modified Eagle's medium (DMEM) (Hyclone, USA) supplemented with 10% fetal bovine serum (FBS, Gibco). One day before infection, approximately 1×10^5 cells were seeded in each well of 24-well plates (Costar, USA), and incubated at 37 °C in a 5% CO₂ atmosphere overnight. The cells were infected at a multiplicity of infection (MOI) of 10:1 and the 24-well plate was centrifuged at $500 \times g$ for 3 min. The bacterial cell mixtures were then incubated at 37 °C in 5% CO₂ for 2 h. Following incubation, each well was washed twice with 500 µL PBS and medium containing 200 µg/mL Gentamicin and 40 µg/mL Lysostaphin was added to kill the bacteria external to the monolayer cells. The plate was then incubated at 37 °C in 5% CO₂ for 30 min, followed by twice washes with 500 µL PBS. The monolayer cells were subsequently lysed with 200 µL 0.1% Triton X-100 for 20 min at room temperature, and were then diluted with PBS and plated on TSB-agar plates to determine the number of intracellular bacteria (Colony-Forming Units, CFU).

Measurement and of carotenoid pigment. Colonies of *S. aureus* USA300 were cultured in TSB or TSB supplemented with 2 mg/mL nicotine at 37 °C for 24 h with shaking. The bacterial cells were thereafter collected by centrifugation and washed three times with distilled water. The formation of carotenoid pigment by bacterial cells of the same wet weight was established visually.

Quantification of carotenoid pigment. *S. aureus* USA300 cells were cultured in TSB or TSB supplemented with 2 mg/mL nicotine at 37°C for 24 h with shaking. Cells were harvested by centrifugation (10000 × g, 2 min), and then washed twice with PBS, following which, 100% methanol was added to extract staphyloxanthin and carotenoids in a water bath at 55°C for 5 min. The resulting methanol extract liquid was centrifuged and the supernatant containing carotenoid pigment was then quantified by estimating the OD at 462 nm using a microplate reader (BioRAD, USA).

Data analysis. Data are presented as the mean ± standard deviation. Comparison between two groups was made using unpaired two-tailed *t*-tests. One-way ANOVA followed by Bonferroni's post hoc test was applied to compare between three or more groups. Prism 5 (GraphPad Software, Inc, CA, USA) was used for statistical analysis. Statistical significance was defined as a two-tailed *P* value < 0.05.

Received: 2 August 2019; Accepted: 10 December 2019;

Published online: 27 December 2019

References

1. Varshney, R. & Lee, J. T. Current trends in topical therapies for chronic rhinosinusitis: update and literature review. *Expert Opin Drug Deliv.* **14**, 257–271 (2017).
2. Tan, B. K., Schleimer, R. P. & Kern, R. C. Perspectives on the etiology of chronic rhinosinusitis. *Curr. Opin Otolaryngol Head Neck Surg.* **18**, 21–26 (2010).
3. Rabin, N. *et al.* Biofilm formation mechanisms and targets for developing antibiofilm agents. *Future Med. Chem.* **7**, 493–512 (2015).
4. Parsek, M. R. & Singh, P. K. Bacterial biofilms: an emerging link to disease pathogenesis. *Annu Rev Microbiol.* **57**, 677–70 (2003).
5. Cryer, J., Schipor, I., Perloff, J. R. & Palmer, J. N. Evidence of bacterial biofilms in human chronic sinusitis. *ORL J. Otorhinolaryngol Relat Spec.* **66**, 155–158 (2004).
6. Warren, C. W. *et al.* Global youth tobacco surveillance, 2000–2007. *MMWR Surveill Summ.* **57**, 1–28 (2008).
7. Giovino, G. A. *et al.* Tobacco use in 3 billion individuals from 16 countries: an analysis of nationally representative cross-sectional household surveys. *The Lancet.* **380**, 668–679 (2012).
8. Lieu, J. E. & Feinstein, A. R. Confirmations and surprises in the association of tobacco use with sinusitis. *Arch. Otolaryngol Head Neck Surg.* **126**, 940–946 (2000).
9. Ebbert, J. O., Croghan, I. T., Schroeder, D. R., Murawski, J. & Hurt, R. D. Association between respiratory tract diseases and secondhand smoke exposure among never smoking flight attendants: a cross-sectional survey. *Environ Health.* **6**, 28 (2007).
10. Kulkarni, R. *et al.* Cigarette smoke increases *Staphylococcus aureus* biofilm formation via oxidative stress. *Infect Immun.* **80**, 3804–3811 (2012).
11. Cockeran, R. *et al.* Exposure of a 23F serotype strain of *Streptococcus pneumoniae* to cigarette smoke condensate is associated with selective upregulation of genes encoding the two-component regulatory system 11 (TCS11). *Biomed Res. Int.* **2014**, 976347 (2014).
12. Mutepe, N. D. *et al.* Effects of cigarette smoke condensate on pneumococcal biofilm formation and pneumolysin. *Eur Respir J.* **41**, 392–395 (2013).
13. Baboni, F. B., Guariza Filho, O., Moreno, A. N. & Rosa, E. A. R. Influence of cigarette smoke condensate on cariogenic and candidal biofilm formation on orthodontic materials. *Am J. Orthod Dentofacial Orthop.* **138**, 427–434 (2010).
14. Goldstein-Daruech, N. *et al.* Tobacco smoke mediated induction of sinonasal microbial biofilms. *PLoS One.* **6**, e15700 (2011).
15. Hutcherson, J. A., Scott, D. A. & Bagaitkar, J. Scratching the surface - tobacco-induced bacterial biofilms. *Tob Induc Dis.* **13**, 1 (2015).
16. Singhal, D., Foreman, A., Jervis-Bardy, J. & Wormald, P. J. *Staphylococcus aureus* biofilms: Nemesis of endoscopic sinus surgery. *Laryngoscope.* **121**, 1578–1583 (2011).
17. Huang, R., Li, M. & Gregory, R. L. Effect of nicotine on growth and metabolism of *Streptococcus* mutants. *Eur J. Oral Sci.* **120**, 319–325 (2012).
18. Huang, R., Li, M. & Gregory, R. L. Nicotine promotes *Streptococcus mutans* extracellular polysaccharide synthesis, cell aggregation and overall lactate dehydrogenase activity. *Arch Oral Biol.* **60**, 1083–1090 (2015).
19. Lan, L. *et al.* Golden pigment production and virulence gene expression are affected by metabolisms in *Staphylococcus aureus*. *J. Bacteriol.* **92**, 3068–3077 (2010).
20. Boles, B. R. & Horswill, A. R. Agr-mediated dispersal of *Staphylococcus aureus* biofilms. *PLoS Pathog.* **4**, e1000052 (2008).
21. Yarwood, J. M., Bartels, D. J., Volper, E. M. & Greenberg, E. P. Quorum sensing in *Staphylococcus aureus* biofilms. *J. Bacteriol.* **186**, 1838–1850 (2004).
22. Jenul, C. & Horswill, A. R. Regulation of *Staphylococcus aureus* virulence. *Microbiol Spectr.* **6**, GPP3-0031-2018 (2018).
23. Li, M. *et al.* Effect of nicotine on dual-species biofilms of *Streptococcus mutans* and *Streptococcus sanguinis*. *FEMS Microbiol Lett.* **350**, 125–132 (2014).
24. Huang, R. *et al.* Effects of Nicotine on *Streptococcus gordonii* growth, biofilm formation, and cell aggregation. *Appl Environ Microbiol.* **80**, 7212–7218 (2014).
25. Wu, Y. *et al.* Nicotine Enhances *Staphylococcus epidermidis* biofilm formation by altering the bacterial autolysis, extracellular DNA releasing, and polysaccharide intercellular adhesion production. *Front Microbiol.* **29**, 2575 (2018).
26. Temple, D. J. The absorption of nicotine from tobacco snuff through the nasal mucosa. *Arch Pharm. (Weinheim).* **309**, 984–987 (1976).
27. Gotz, F. *Staphylococcus* and biofilms. *Mol Microbiol.* **43**, 1367–1378 (2002).
28. Cogo, K. *et al.* The effects of nicotine and cotinine on *Porphyromonas gingivalis* colonisation of epithelial cells. *Arch Oral Biol.* **54**, 1061–1067 (2009).
29. Lacombe, A. *et al.* Cigarette smoke exposure redirects *Staphylococcus aureus* to a virulence profile associated with persistent infection. *Sci. Rep.* **9**, 10798 (2019).
30. McCourt, J. *et al.* Fibronectin-binding proteins are required for biofilm formation by community-associated methicillin-resistant *Staphylococcus aureus* strain LAC. *FEMS Microbiol Lett.* **353**, 157–164 (2014).
31. Cheng, A. G., Missiakas, D. & Schneewind, O. The giant protein Ehb is a determinant of *Staphylococcus aureus* cell size and complement resistance. *J. Bacteriol.* **196**, 971–981 (2014).
32. Bao, Y., Zhang, X., Jiang, Q., Xue, T. & Sun, B. Pfs promotes autolysis-dependent release of eDNA and biofilm formation in *Staphylococcus aureus*. *Med Microbiol Immunol.* **204**, 215–226 (2015).
33. Ratner, A. J. *et al.* Modulation of eDNA Release and Degradation Affects *Staphylococcus aureus* Biofilm Maturation. *PLoS One.* **4**, e5822 (2009).
34. McEachern, E. K. *et al.* Analysis of the effects of cigarette smoke on staphylococcal virulence phenotypes. *Infect Immun.* **83**, 2443–2452 (2015).
35. Okano, M. *et al.* Cellular responses to *Staphylococcus aureus* alpha-toxin in chronic rhinosinusitis with nasal polyps. *Allergol Int.* **63**, 563–573 (2014).

36. Novick, R. P. Autoinduction and signal transduction in the regulation of staphylococcal virulence. *Mol Microbiol.* **48**, 1429–1449 (2003).
37. Allesen-Holm, M. *et al.* A characterization of DNA release in *Pseudomonas aeruginosa* cultures and biofilms. *Molecular Microbiolog.* **59**, 1114–1128 (2006).
38. Qin, Z. *et al.* Role of autolysin-mediated DNA release in biofilm formation of *Staphylococcus epidermidis*. *Microbiology.* **153**, 2083–2092 (2007).
39. Diep, B. A. *et al.* Complete genome sequence of USA300, an epidemic clone of community-acquired methicillin-resistant *Staphylococcus aureus*. *Lancet.* **367**, 731–739 (2006).

Acknowledgements

This work was funded by the National Nature Science Foundation of China for Young Scholars (No. 81300810), the National Natural Science Foundation of China (No. 81970855), the Shanghai Young Doctor Training Program (No. 20141057), the National Natural Science Foundation of China (No. 81671982), Zhejiang Provincial Natural Science Foundation of China (grant number LY16H190006), and the National Natural Science Foundation of China (No. 81991532), National Science and Technology Major Project of China (2018ZX10734401-004), National Mega-project for Innovative Drugs (2019ZX09721001) and Zhengyi Scholar Program of Fudan University.

Author contributions

Le Shi and Chen Yang prepared figures 3–9 and Yue Ma prepared figures 1 and 2. Qingzhao Zhang, Xiaoyi Zhu, and Yingjie Yan analyzed the data. Wei Huang and Tao Zhu contributed to problem solving during experiments. Jiaxue Wang funded a part of the study. Yang Wu and Keqing Zhao wrote the manuscript. Di Qu and Chunquan Zheng supervised the study.

Competing interests

The authors declare no competing interests.

Additional information

Correspondence and requests for materials should be addressed to D.Q., C.-q.Z. or K.-Q.Z.

Reprints and permissions information is available at www.nature.com/reprints.

Publisher's note Springer Nature remains neutral with regard to jurisdictional claims in published maps and institutional affiliations.



Open Access This article is licensed under a Creative Commons Attribution 4.0 International License, which permits use, sharing, adaptation, distribution and reproduction in any medium or format, as long as you give appropriate credit to the original author(s) and the source, provide a link to the Creative Commons license, and indicate if changes were made. The images or other third party material in this article are included in the article's Creative Commons license, unless indicated otherwise in a credit line to the material. If material is not included in the article's Creative Commons license and your intended use is not permitted by statutory regulation or exceeds the permitted use, you will need to obtain permission directly from the copyright holder. To view a copy of this license, visit <http://creativecommons.org/licenses/by/4.0/>.

© The Author(s) 2019